Heliyon 9 (2023) e16926

Contents lists available at ScienceDirect

Heliyon

journal homepage: www.cell.com/heliyon

High throughput LC/ESI-MS/MS method for simultaneous analysis of 20 oral molecular-targeted anticancer drugs and the active metabolite of sunitinib in human plasma

Tensei Hirasawa [a], Masafumi Kikuchi [a,b,*], Shinya Takasaki [b], Masaki Kumondai [b], Yu Sato [b], Toshihiro Sato [b], Eishi Imoto [c], Yoshihiro Hayakawa [c], Masamitsu Maekawa [a,b], Nariyasu Mano [a,b]

[a] Faculty of Pharmaceutical Sciences, Tohoku University, 6-3 Aoba, Aramaki, Aoba-ku, Sendai 980-8578, Japan
[b] Department of Pharmaceutical Sciences, Tohoku University Hospital, 1-1 Seiryo-machi, Aoba-ku, Sendai 980-8574, Japan
[c] Shimadzu Corporation, 1 Nishinokyo Kuwabara-cho, Nakagyo-ku, Kyoto 604-8511, Japan

ARTICLE INFO

Keywords:
Oral molecular-targeted drug
LC/ESI-MS/MS
Collision energy defects
In-source collision-induced dissociation
Secondary product ion selected reaction monitoring
Isotopologue selected reaction monitoring

ABSTRACT

Many types of oral molecular-targeted anticancer drugs are clinically used in cancer genomic medicine. Combinations of multiple molecular-targeted anticancer drugs are also being investigated, expecting to prolong the survival of patients with cancer. Therapeutic drug monitoring of oral molecular-targeted drugs is important to ensure efficacy and safety. A liquid chromatography/electrospray ionization-tandem mass spectrometry (LC/ESI-MS/MS) has been used for simultaneous determination of these drugs in human plasma. However, the sensitivity of mass spectrometers and differences in the therapeutic range of drugs have rendered the development of simultaneous LC/ESI-MS/MS methods difficult. In this study, a simultaneous quantitative method for 20 oral molecular-targeted anticancer drugs and the active metabolite of sunitinib was developed based on the results of linear range shifts of the calibration curves using four ion abundance adjustment techniques (collision energy defects, in-source collision-induced dissociation, secondary product ion selected reaction monitoring, and isotopologue selected reaction monitoring). The saturation of the detector for the seven analytes was resolved by incorporating optimal ion abundance adjustment techniques. Furthermore, the reproducibility of this method was confirmed in validation tests, and plasma from patients was measured by this method to demonstrate its usefulness in actual clinical practice. This analytical method is expected to make a substantial contribution to the promotion of personalized medicine in the future.

1. Introduction

Cancer genomic medicine is being promoted as a therapy that selects drugs according to therapeutic target genes of patients with cancer and their characteristics through genetic mutations of cancer tissue [1]. Even in the same cancer type, mutations of therapeutic target genes (driver mutation) are diverse. In Japanese patients with lung adenocarcinoma, the frequency of driver mutation is about 53% for epidermal growth factor receptor (EGFR) mutation, 10% for Kirsten rat sarcoma viral oncogene homolog mutation, 3% for

* Corresponding author. Faculty of Pharmaceutical Sciences, Tohoku University, 6-3 Aoba, Aramaki, Aoba-ku, Sendai 980-8578, Japan.
E-mail address: masafumi.kikuchi.b2@tohoku.ac.jp (M. Kikuchi).

https://doi.org/10.1016/j.heliyon.2023.e16926
Received 14 April 2023; Received in revised form 20 May 2023; Accepted 1 June 2023
Available online 2 June 2023

anaplastic lymphoma kinase fusion gene, and 3% for human epidermal growth factor receptor 2 mutation. Rearranged during transfection fusion gene has been reported to be approximately 2% [2]. High therapeutic efficacy can be obtained with oral molecular-targeted anticancer drugs when therapeutic targets, such as gene mutations are identified in patients with cancer. Therefore, a variety of cancer drug therapies using oral molecular-targeted anticancer drugs corresponding to therapeutic target gene mutations are being implemented in cancer genomic medicine [3].

Many oral molecular-targeted anticancer drugs have been developed to enable cancer therapy in an outpatient setting [4]. To treat patients with cancer and multiple identified target gene mutations and to avoid drug resistance owing to feedback activation of cancer cell signaling, the combination of oral molecular-targeted anticancer drugs has recently been suggested to be useful [5–9]. Lenvatinib in combination with gefitinib improved the therapeutic efficacy in patients with hepatocellular carcinoma with high expression of EGFR [7]. Accordingly, cancer genomic medicine using oral molecular-targeted anticancer drugs is diverse and complex. In addition, individualized dosing design of anticancer drugs based on blood concentrations is emphasized because many oral molecular-targeted anticancer drugs show large inter-individual variability, and a correlation is present between the exposure dose and therapeutic efficacy or side effects [10,11]. Imatinib, a drug for chronic myeloid leukemia (CML), is effective in maintaining trough concentrations of imatinib above 1002 ng/mL, although individual blood levels widely vary owing to differences in the expression of metabolic enzymes or transporters and interactions with concomitant medications [12,13]. Therapeutic drug monitoring (TDM) for imatinib and sunitinib is performed in clinical practice in Japan. Furthermore, information on exposure, therapeutic efficacy, and side effects of many oral molecular-targeted anticancer drugs need to be collected, and studies on pharmacokinetics/pharmacodynamics analysis are underway [14]. Hence, a quantification method that can easily and quickly analyze the concentration of each oral molecular-targeted anticancer drug in human plasma is urgently required. A liquid chromatography/electrospray ionization-tandem mass spectrometry (LC/ESI-MS/MS) has been utilized as a suitable method for the simultaneous quantification of multiple analytes [15]. However, the physicochemical properties and therapeutic concentration range of each analyte greatly differ. To analyze each analyte using the same method, their quantification range must be kept within the range where the linearity of the signal intensity at the detector can be ensured. Although the sample is usually diluted or concentrated to ensure the linearity of the calibration curve, this requires complex pretreatment and multiple measurements. In fact, the pretreatment process in the simultaneous quantification method becomes more complicated as the number of analytes increases [16–18]. Therefore, high throughput in clinical practice has not been ensured. Furthermore, simultaneous quantification methods for drugs, such as ibrutinib and pazopanib, which have a large difference of more than 100,000-fold in the required concentration range, have not been reported.

We have previously investigated techniques for easily adjusting the number of ions introduced into MS. In addition to collision energy defect (CED), which utilizes collision energy (CE), in-source collision-induced dissociation (in-source CID), secondary product ion selected reaction monitoring (*s*-SRM), and isotopologue SRM (*i*-SRM) have been reported [19–22]. In-source CID is a technique for limiting the amounts of excess ions by regulating the voltage behind the orifice to promote fragmentation of any protonated ion by colliding and breaking up with air molecules and has been used for quantitative analysis of oral molecular-targeted anticancer drugs [23–27]. *s*-SRM simultaneously monitors product ions with different relative intensities, whereas *i*-SRM monitors product ions that are usually detected in one mass unit by quadrupole MS [21,22]. Many analytes with different physicochemical properties and therapeutic concentration ranges can be simultaneously measured by using these four ion abundance adjustment techniques. Therefore, we investigated the effects of these four techniques on 20 oral molecular-targeted anticancer drugs and the active metabolite of sunitinib [28].

In this study, we attempted to examine the ESI-MS/MS and LC conditions for the simultaneous quantification system based on the results of four ion abundance adjustment techniques. The reliability of the developed method was verified through a validation test. Furthermore, to confirm the clinical usefulness of the method, we measured blood drug concentrations in samples obtained from patients with cancer, compared the quantitative values with those previously reported, and evaluated the analytical performance of the method.

2. Materials and methods

2.1. Chemical and reagents

Afatinib, bosutinib, dacomitinib, gefitinib, ibrutinib, imatinib, lapatinib, lenvatinib, nilotinib, nintedanib, osimertinib, ponatinib, regorafenib, vandetanib, afatinib-$^{2}H_{6}$ (internal standard (IS)), bosutinib-$^{2}H_{8}$, dasatinib-$^{2}H_{8}$, gefitinib-$^{2}H_{6}$, ibrutinib-$^{2}H_{5}$, lapatinib-$^{2}H_{4}$, nilotinib-$^{2}H_{6}$, nintedanib-^{13}C–$^{2}H_{3}$, and pazopanib-$^{2}H_{6}$ were purchased from Cayman Chemical Company (Ann Arbor, MI, USA). Axitinib, erlotinib, sorafenib, sunitinib, *N*-desethyl sunitinib, axitinib-$^{2}H_{3}$, erlotinib-$^{2}H_{6}$, imatinib-$^{2}H_{8}$, sorafenib-$^{2}H_{3}$, and sunitinib-$^{2}H_{4}$ were purchased from Toronto Research Chemicals (Toronto, Canada). Dasatinib was purchased from LC Laboratories (Woburn, MA, USA). Dacomitinib-$^{2}H_{10}$, lenvatinib-$^{2}H_{5}$, osimertinib-^{13}C–$^{2}H_{3}$, ponatinib-$^{2}H_{8}$, regorafenib-^{13}C–$^{2}H_{3}$, and vandetanib-^{13}C–$^{2}H_{6}$ were purchased from Alsachim (Illkirch-Graffenstaden, France). Pazopanib was purchased from Synkinase (Melbourne, Victoria, Australia). High performance liquid chromatography (HPLC)-grade ammonium formate, formic acid, and methanol were purchased from the Fujifilm Wako Pure Chemical Corporation (Osaka, Japan). HPLC-grade acetonitrile was purchased from the Kanto Chemical Corporation (Tokyo, Japan). Ultrapure water was obtained using a Puric-α purification system (Organo Corporation, Tokyo, Japan) and was used for LC/ESI-MS/MS analysis. All other chemicals used were of the highest commercially available purity. Heparinized human plasma was supplied by Cosmo Bio Co. Ltd. (Tokyo, Japan).

2.2. LC/ESI-MS/MS conditions

The LC/ESI-MS/MS system was performed using an LCMS-8050 triple quadrupole mass spectrometer coupled with a Nexera X2 UHPLC system (Shimadzu, Kyoto, Japan). All data acquisition and processing were performed using LabSolutions (Shimadzu). The Nexera X2 UHPLC system consisted of a vacuum degasser, two solvent delivery systems, an autosampler, and a column oven. Chromatographic separation was achieved using a YMC-Triart C18 metal-free column (2.1 mm i. d. × 50 mm, 3 μm; YMC, Kyoto, Japan). The column temperature was maintained at 40 °C, and the samples were kept at 4 °C. The flow rate was set at 0.45 mL/min, and the injection volume was 6 μL for analysis. Mobile phases A and B comprised 10 mM aqueous ammonium formate (A) adjusted to pH 3.6 and 10 mM of ammonium formate-methanol (B). The gradient program was as follows: B conc. 0–0.8 min, 40%–50%; 0.8–2.4 min, 50%–57%; 2.4–2.6 min 57%–75%; 2.6–3.8 min, 75%–80%; 3.8–4.0 min, 80%–100%, 4.0–4.3 min, 100%; 4.31–5.0 min, 40%. The LCMS-8050 was equipped with an ESI source operating in the positive-ion detection mode. The conditions for mass spectrometry (MS) analysis were as follows: probe voltage, 4000 V; desolvation line temperature, 250 °C; block heater temperature, 400 °C; interface temperature, 300 °C; nebulizing gas flow, 3 L/min; drying gas, 10 L/min; and heating gas flow, 10 L/min.

2.3. Preparation of calibration standards, quality control, and IS solutions

Stock solutions of 0.1–1 mg/mL in methanol or methanol-dimethyl sulfoxide (50:50, v/v) were prepared and stored at −80 °C. The stock solutions were mixed and diluted with human plasma to prepare calibration standards (CS) and quality controls (QC), which were stored at −20 °C. The details of CS and QC samples are shown in Table 1. The stock solutions were mixed and diluted with acetonitrile/methanol (90:10, v/v) to prepare IS solutions; 10 ng/mL for axitinib-$^{2}H_3$, dasatinib-$^{2}H_8$, ibrutinib-$^{2}H_5$, nintedanib-^{13}C–$^{2}H_3$, ponatinib-$^{2}H_8$, and sunitinib-$^{2}H_4$, 50 ng/mL for afatinib-$^{2}H_6$, bosutinib-$^{2}H_8$, dacomitinib-$^{2}H_{10}$, gefitinib-$^{2}H_6$, lenvatinib-$^{2}H_5$, osimertinib-^{13}C–$^{2}H_3$, regorafenib-^{13}C–$^{2}H_3$, and vandetanib-^{13}C–$^{2}H_6$, 300 ng/mL for erlotinib-$^{2}H_6$, imatinib-$^{2}H_8$, lapatinib-$^{2}H_4$, nilotinib-$^{2}H_6$, pazopanib-$^{2}H_6$, and sorafenib-$^{2}H_3$. All prepared IS solutions were stored at −20 °C.

Table 1
Concentration of 20 oral molecular-targeted anticancer drugs and the active metabolite of sunitinib in the calibration standards (CS) and quality control (QC) samples.

Analytes	Group	CS (ng/mL)		QC (ng/mL)	
Ibrutinib	Low	CS1:	0.3	LLOQ:	0.3
Nintendanib		CS2:	3	LQC:	0.9
Ponatinib		CS3:	15	MQC:	120
		CS4:	75	HQC:	240
		CS5:	225		
		CS6:	300		
Axitinib	Low	CS1:	1	LLOQ:	1
Dasatinib		CS2:	3	LQC:	3
Sunitinib		CS3:	15	MQC:	120
N-Desethyl sunitinib		CS4:	75	HQC:	240
		CS5:	225		
		CS6:	300		
Afatinib	Middle	CS1:	1	LLOQ:	1
Bosutinib		CS2:	10	LQC:	3
Dacomitinib		CS3:	50	MQC:	1200
Gefitinib		CS4:	750	HQC:	2400
Lenvatinib		CS5:	2250		
Osimertinib		CS6:	3000		
Regorafenib					
Vandetanib					
Erlotinib	High	CS1:	30	LLOQ:	30
Imatinib		CS2:	300	LQC:	90
Lapatinib		CS3:	1500	MQC:	4000
Nilotinib		CS4:	2500	HQC:	8000
Sorafenib		CS5:	7500		
		CS6:	10,000		
Pazopanib	High	CS1:	30	LLOQ:	30
		CS2:	300	LQC:	90
		CS3:	1500	MQC:	20,000
		CS4:	2500	HQC:	40,000
		CS5:	7500		
		CS6:	50,000		

LLOQ, lower limit of quantification; LQC, low quality control; MQC, medium quality control; HQC, high quality control.

2.4. Sample pre-treatment

Eighty microliters of each of the IS and acetonitrile-methanol (9:1, v/v) solutions were added to 40 μL of the plasma sample contained in a 1.5 mL microcentrifuge tube. The mixture was vortexed for 5 min and centrifuged at 14,000×*g* for 10 min at 4 °C. After centrifugation, 6 μL of the supernatant was injected into the analytical system.

2.5. CED, in-source CID, s-SRM, i-SRM

We adjusted the ion abundance of compounds that exhibited detector saturation based on the effects of the four techniques (CED, in-source CID, *s*-SRM, and *i*-SRM) as previously reported [28].

2.6. Validation

This method was validated according to the US Food and Drug Administration guideline for the validation of bioanalytical assays [29]. Specificity and selectivity, linearity and lower limit of quantitation (LLOQ), precision and accuracy, matrix effect, carry-over, and stability tests were performed for validation.

2.6.1. Specificity and selectivity

To investigate whether endogenous matrix constituents interfered with the assay, blank plasma from six individuals containing neither analyte nor IS, samples containing the LLOQ of analyte and IS were prepared and analyzed.

2.6.2. Linearity

The linearity of the assay was investigated by analyzing six CS samples in six independent analytical runs. Regression of the calibration curves was calculated by the linear weighted least-squares method with a weighting factor of $1/x^2$. Moreover, the determination coefficient (R^2) was at least 0.990.

2.6.3. Precision and accuracy

The intra-day precision and accuracy were assessed by analyzing six replicate QC samples at four different levels (LLOQ, low quality control (LQC), medium quality control (MQC), and high quality control (HQC)) on the same day. The inter-day precision and accuracy were estimated by analyzing the QC samples in six analytical runs.

2.6.4. Matrix effect

To investigate whether the endogenous matrix components interfered with the assay, six different blank plasma samples were used to measure and analyze two levels (LQC and HQC) in sextuple. In addition, the IS-normalized matrix factor (MF) was evaluated by comparing the peak areas of the analytes and IS obtained from the plasma solvent sample with those obtained by measuring the same amount of the standard solution.

2.6.5. Carry-over

Carry-over was examined using a blank sample immediately injected after the highest standard point and an LLOQ sample. The area ratio of the blank sample to the LLOQ was determined.

2.6.6. Stability

The stability of oral molecular-targeted drugs in human plasma was investigated using LQC, MQC, and HQC samples after storage at room temperature (25 °C) for 4 h or 4 °C for 24 h. The freeze and thaw stability was determined after three freeze-thaw cycles (from −80 to 25 °C).

2.7. Clinical application

This new method was applied to the pharmacokinetic study approved by the institutional review board of the Graduate School of Medicine at Tohoku University (No. 2020-1-1100, 2020-1-618, 2021-1-189, and 2021-1-710). After obtaining written informed consent from the patients, the blood samples were collected. The heparinized blood was centrifuged at 1580×*g* for 10 min at 4 °C. The obtained plasma samples were collected and stored at −20 °C until analysis.

3. Results and discussion

3.1. Method development

To achieve high-throughput analysis in a clinical setting without the need for complicated switching of columns and mobile phases, we selected YMC-Triart C18 metal-free (2.1 mm i. d. × 50 mm, 3 μm) as the analytical column, 10 mM ammonium formate adjusted to pH 3.6, and 10 mM ammonium formate-methanol as mobile phase A and B, respectively. Even if highly selective analysis by MS/MS is possible, inadequate separation by LC can lead to ion suppression and crosstalk between peaks with close retention times. Therefore,

the gradient condition with a more gradual gradient slope was investigated, resulting in a good separation with a chromatographic run time of 5 min, as shown in Fig. 1. In addition, to ensure sensitivity in the low concentration range, the injection volume was set to 6 μL, and the LC condition was constructed. Imatinib and some other compounds strongly bind to many metals, such as copper and nickel [30,31]. To avoid poor quantitation owing to adsorption on metal parts of the LC system, not only the metal-free column but also the LC piping was changed from metal to PEEK tubing.

Optimization of all analytes was performed using LCMS-8050 as the mass spectrometer. The transition and voltage values that give the highest intensity for oral molecular-targeted anticancer drugs, active metabolite of sunitinib, and IS were examined for Q1/Q3 pre bias and CE. First, mass spectra of the compounds and IS were obtained by the flow injection analysis method, all protonated ions were detected as base peaks, and each SRM transition was determined. The base peak ion of each compound was used as the precursor ion, and the product ion obtained with the highest intensity was examined by changing the voltage of CE from −5 to −50 V every 1 V. For Q1 pre bias and Q3 pre bias, the voltage was changed every 2 V between −5 and −50 V to set the optimum values. The optimized SRM parameters are shown in Table 2.

The calibration ranges of the 20 oral molecular-targeted anticancer drugs and a metabolite were classified into three groups: low (0.3−300 ng/mL), middle (1−3000 ng/mL), and high (30−10,000 ng/mL) based on the information on patient blood levels during cancer drug therapy. For low group drugs, concentrations of axitinib, dasatinib, sunitinib, and *N*-desethyl sunitinib ranged from 1 to 300 ng/mL, and for pazopanib in the high group, concentrations ranged from 30 to 50,000 ng/mL.

3.2. Application of the ion adjustment method

The linear range of the calibration curves under optimized SRM conditions was investigated for the determined calibration ranges and showed detector saturation for erlotinib, osimertinib, imatinib, lapatinib, nilotinib, pazopanib, and sorafenib (Fig. 2). Therefore, it was necessary to adjust the ion amount for these compounds based on the results of previous studies [28].

In-source CID was selected as the first choice for ion abundance adjustment because it has a substantial effect on the linear range of the calibration curves, and it prevents the introduction of excess ions into the mass separation section; thereby, ensuring stable measurements over the long term. In-source CID was applied to the 7 compounds listed above. For the four compounds, erlotinib, osimertinib, imatinib, and lapatinib, setting the Q-array bias to 120, 130, 170, and 170 V, respectively, avoided detector saturation and resulted in good calibration curves. Although lapatinib was less effective in adjusting the ion abundance by in-source CID, it was possible to slightly shift the linear range of the calibration curve under high Q-array bias of 170 V [28]. On the other hand, nilotinib, pazopanib, and sorafenib required adjustment by other methods than in-source CID. Therefore, we selected two or three candidates from the three ion abundance adjustment techniques (CED, *s*-SRM, and *i*-SRM), and examined their linearity of the calibration curve and precision at LLOQ (Table 3). As a result, the application of in-source CID to 4 compounds (erlotinib, osimertinib, imatinib, and lapatinib), *s*-SRM to pazopanib, and *i*-SRM to 2 compounds (nilotinib and sorafenib) solved the problem of detector saturation. The final SRM conditions for the 7 compounds to which the ion abundance adjustment techniques were adapted are shown in Table 4, and the measurement conditions were determined under optimized conditions for the remaining compounds.

3.3. Validation

We evaluated the specificity and selectivity of the method by comparison of representative SRM chromatograms of blank human

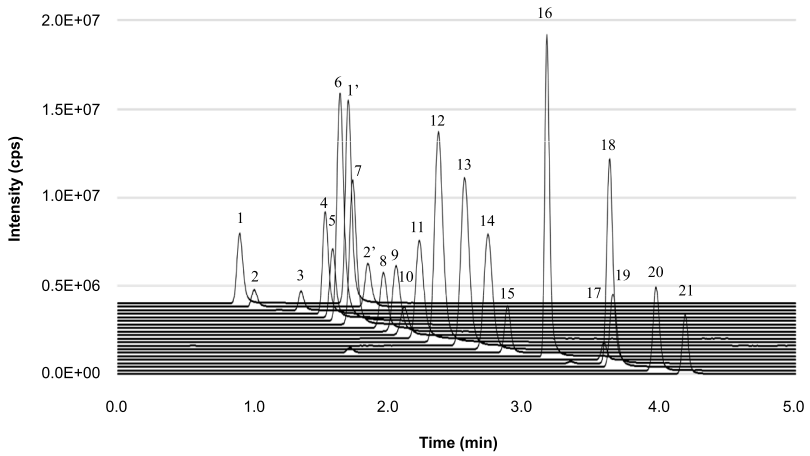

Fig. 1. Selected reaction monitoring chromatograms of the analytes in human plasma spiked with standard solution at a concentration of 100 ng/mL 1, *N*-desethyl sunitinib (*E*-isomer); 1′, *N*-desethyl sunitinib (*Z*-isomer); 2, Sunitinib (*E*-isomer); 2′, Sunitinib (*Z*-isomer); 3, Pazopanib; 4, Imatinib; 5, Dasatinib; 6, Gefitinib; 7, Vandetanib; 8, Lenvatinib; 9, Afatinib; 10, Dacomitinib; 11, Bosutinib; 12, Osimertinib; 13, Erlotinib; 14, Nintedanib; 15, Axitinib; 16, Ponatinib; 17, Ibrutinib; 18, Nilotinib; 19, Lapatinib; 20, Sorafenib; 21, Regorafenib.

Table 2
Selected reaction monitoring parameters for 20 oral molecular-targeted anticancer drugs, active metabolite of sunitinib, and internal standards.

Analytes	Retention time (min)	SRM transition	Q1 pre bias (V)	CE (V)	Q3 pre bias (V)
Afatinib	2.05	*m/z* 486.4 → 371.0	−26	−29	−18
Afatinib-$^{2}H_{6}$	2.04	*m/z* 492.4 → 371.1	−10	−28	−18
Axitinib	2.87	*m/z* 387.4 → 356.2	−20	−19	−48
Axitinib-$^{2}H_{3}$	2.87	*m/z* 390.4 → 356.2	−12	−20	−18
Bosutinib	2.22	*m/z* 530.0 → 141.1	−26	−26	−14
Bosutinib-$^{2}H_{8}$	2.20	*m/z* 538.0 → 149.2	−26	−25	−10
Dacomitinib	2.11	*m/z* 470.4 → 385.1	−26	−25	−28
Dacomitinib-$^{2}H_{10}$	2.09	*m/z* 480.5 → 385.2	−26	−27	−18
Dasatinib	1.59	*m/z* 488.4 → 401.1	−26	−29	−42
Dasatinib-$^{2}H_{8}$	1.58	*m/z* 496.4 → 406.2	−26	−31	−20
Erlotinib	2.55	*m/z* 394.4 → 278.1	−20	−32	−50
Erlotinib-$^{2}H_{6}$	2.49	*m/z* 400.4 → 278.1	−22	−32	−20
Gefitinib	1.64	*m/z* 447.4 → 128.1	−24	−24	−24
Gefitinib-$^{2}H_{6}$	1.62	*m/z* 453.4 → 134.1	−24	−23	−24
Ibrutinib	3.58	*m/z* 441.4 → 138.1	−24	−28	−50
Ibrutinib-$^{2}H_{5}$	3.56	*m/z* 446.5 → 138.2	−24	−27	−14
Imatinib	1.53	*m/z* 494.5 → 394.2	−26	−26	−44
Imatinib-$^{2}H_{8}$	1.52	*m/z* 502.1 → 394.2	−50	−27	−30
Lapatinib	3.65	*m/z* 581.4 → 365.1	−18	−36	−38
Lapatinib-$^{2}H_{4}$	3.62	*m/z* 585.5 → 365.1	−8	−36	−18
Lenvatinib	1.96	*m/z* 427.3 → 370.1	−22	−29	−26
Lenvatinib-$^{2}H_{5}$	1.94	*m/z* 432.4 → 370.1	−24	−28	−18
Nilotinib	3.62	*m/z* 530.4 → 289.1	−28	−29	−20
Nilotinib-$^{2}H_{6}$	3.60	*m/z* 536.5 → 295.2	−16	−29	−20
Nintedanib	2.73	*m/z* 540.1 → 113.1	−26	−27	−12
Nintedanib-^{13}C–$^{2}H_{3}$	2.73	*m/z* 544.5 → 117.2	−30	−26	−20
Osimertinib	2.36	*m/z* 500.5 → 72.1	−10	−31	−12
Osimertinib-^{13}C–$^{2}H_{3}$	2.32	*m/z* 504.5 → 72.1	−28	−26	−12
Pazopanib	1.35	*m/z* 438.4 → 357.3	−24	−30	−26
Pazopanib-$^{2}H_{6}$	1.33	*m/z* 444.4 → 363.2	−24	−30	−18
Ponatinib	3.16	*m/z* 533.5 → 260.2	−26	−31	−44
Ponatinib-$^{2}H_{8}$	3.15	*m/z* 541.5 → 260.1	−28	−28	−18
Regorafenib	4.18	*m/z* 483.3 → 270.1	−26	−34	−48
Regorafenib-^{13}C–$^{2}H_{3}$	4.17	*m/z* 487.3 → 274.1	−26	−34	−30
Sorafenib	3.96	*m/z* 465.3 → 252.1	−26	−32	−46
Sorafenib-$^{2}H_{3}$	3.95	*m/z* 468.3 → 255.1	−26	−32	−18
Sunitinib	1.00, 1.85	*m/z* 399.4 → 283.1	−22	−26	−30
N-Desethyl sunitinib	0.90, 1.70	*m/z* 371.4 → 283.1	−20	−21	−30
Sunitinib-$^{2}H_{4}$	0.99, 1.85	*m/z* 403.5 → 283.1	−22	−28	−14
Vandetanib	1.73	*m/z* 475.3 → 112.2	−26	−25	−12
Vandetanib-^{13}C–$^{2}H_{6}$	1.72	*m/z* 481.4 → 112.2	−26	−23	−20

SRM, selected reaction monitoring; CE, collision energy.

plasma from six individuals with those of human plasma containing the LLOQ of each analyte or IS. Blank human plasma showed no peaks co-eluting and no interference with any of the compounds.

Results of linearity are presented in Table S1 of the supplementary information. The calibration curves of each analyte showed good linearity in the target concentration range, with $R^2 > 0.990$.

Results of intra-/inter-day assays are presented in Table 5. The results showed that the relative errors (RE) and coefficients of variation (CV) for intra-day assay were within ±13.8% and 12.2%, respectively (within ±10.5% and 19.1% at the LLOQ). The RE and CV for inter-day assay were within ±13.6% and 13.4%, respectively (within ±13.6% and 18.1% at the LLOQ). This indicates that the method is a quantitative system with sufficient precision and accuracy.

Results of the matrix effect are presented in Table 5 and Fig. 3. The CV for the matrix effect were all within 13.7%. Furthermore, IS-normalized MFs were found to range from 88.0% to 110.8%. Therefore, the matrix effect was acceptable at each QC level for all analytes.

Results of carry-over are presented in Table S2 of the supplementary information. The percentage of carry-over was more than 20% of the LLOQ area for five compounds. Because adsorption on metal piping was considered a possible cause, carry-over was avoided for all analytes by washing the samples with injections of 10 μL of methanol for 3 times [30].

Results of stability are presented in Table 5. The stability of each sample was tested at 25 °C for 4 h, 4 °C for 24 h, and three freeze-thaw cycles. Each compound met the criteria in three freeze-thaw tests, whereas the LQC samples of three compounds, dacomitinib, osimertinib, and pazopanib, showed values outside the criteria for accuracy or precision at 25 °C for 4 h or 4 °C for 24 h. Possible factors include reactions with and adsorption of proteins in plasma, especially, osimertinib, which has been reported by several studies to be unstable in plasma at high temperatures [32–34] The mechanism is the irreversible Michael addition reaction between cysteine and histidine residues of albumin and other proteins in plasma and the α-β unsaturated carbonyl moiety of the osimertinib structure [34]. Adsorption of some tyrosine kinase inhibitors to polymeric polymers has also been reported, and in the case of dacomitinib and

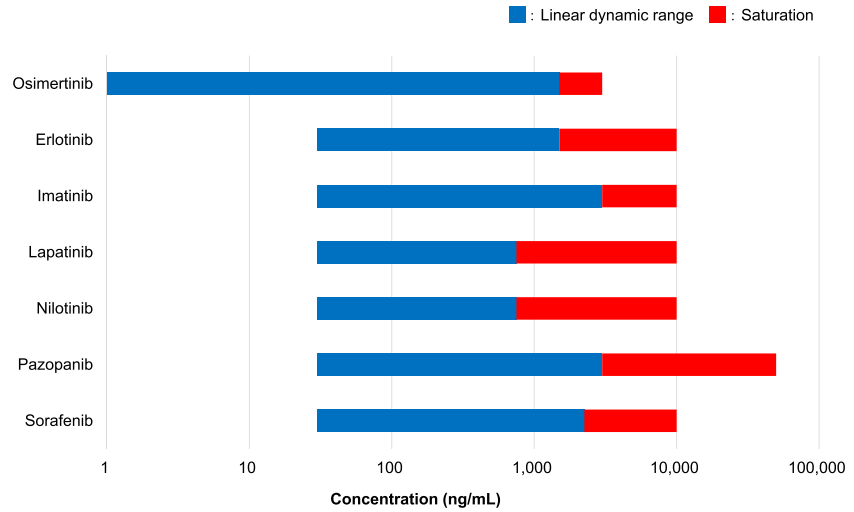

Fig. 2. The linear range of the calibration curves of 7 oral molecular-targeted anticancer drugs (osimertinib, erlotinib, imatinib, lapatinib, nilotinib, pazopanib, and sorafenib).

Table 3
Linearity of the calibration curve and precision at the LLOQ of nilotinib, pazopanib, and sorafenib using ion abundance adjustment techniques.

Compound	Technique	R^2	CV (%, LLOQ)
Nilotinib	*i*-SRM (532.1 > 291.3)	>0.999	6.60
	CED (−55 V)	0.999	6.85
	s-SRM (307.2)	0.996	8.83
Pazopanib	*s*-SRM (342.30)	>0.999	4.44
	CED (−20 V)	0.997	6.81
	i-SRM (440.2 > 343.4)	>0.999	32.6
Sorafanib	*i*-SRM (466.1 > 252.2)	>0.999	2.54
	CED (−50 V)	0.998	19.7

R^2, determination coefficient; CV, coefficient of variation; LLOQ, lower limit of quantification.

Table 4
Final selected reaction monitoring parameters of 7 oral molecular-targeted anticancer drugs.

Analytes	SRM transition	Q1 pre bias (V)	CE (V)	Q3 pre bias (V)	Q-array bias (V)
Erlotinib	*m/z* 394.4 → 278.1	−20	−32	−50	120
Imatinib	*m/z* 494.5 → 394.2	−26	−26	−44	170
Lapatinib	*m/z* 581.4 → 365.1	−18	−36	−38	170
Nilotinib	*m/z* 532.1 → 291.3	−5	−32	−20	0
Osimertinib	*m/z* 500.5 → 72.1	−10	−31	−12	130
Pazopanib	*m/z* 438.2 → 342.3	−28	−48	−16	0
Sorafenib	*m/z* 466.1 → 252.2	−5	−30	−12	0

SRM, selected reaction monitoring; CE, collision energy.

pazopanib, adsorption to the vials may have occurred owing to prolonged storage in the polypropylene vials [35]. Therefore, it is necessary to avoid prolonged storage regardless of temperature and to perform the measurement immediately after thawing.

3.4. Clinical application

The plasma concentrations of 12 analytes obtained from 11 patients with cancer were analyzed using the new analytical method (Fig. S1 of the supplementary information and Table 6).

All analytes were successfully quantified, and their concentrations were within the range of measurement. No remarkable difference was detected in any of the measurement results from those reported in previous reports, and the values were confirmed to be reasonable ranging from the drug administration schedule to the blood collection time [36–45]. Therefore, this method was applied to the measurement of blood concentrations in patients receiving oral molecular-targeted anticancer drugs.

Table 5
Assay performance (n = 6), matrix effect (n = 6), and stability (n = 3) of 20 oral molecular-targeted anticancer drugs and the active metabolite of sunitinib.

Analytes	Control samples	Intra-day		Inter-day		Matrix effect	25 °C, 4 h		4 °C, 24 h		3 times Freeze-thaw	
		RE (%)	CV (%)	RE (%)	CV (%)	CV (%)	RE (%)	CV (%)	RE (%)	CV (%)	RE (%)	CV (%)
Afatinib	LLOQ	10.5	14.8	11.1	2.9	–	–	–	–	–	–	–
	LQC	12.8	12.2	−1.1	8.6	8.5	5.1	1.2	13.9	4.1	−11.6	11.5
	MQC	−1.1	4.5	1.0	8.0	–	−7.6	3.2	−10.8	3.3	−7.6	13.8
	HQC	−3.7	3.7	4.5	2.1	2.8	3.3	2.9	−9.2	8.2	0.6	3.2
Axitinib	LLOQ	5.1	5.6	10.8	10.5	–	–	–	–	–	–	–
	LQC	6.7	4.2	−9.5	1.8	12.6	−8.8	6.9	−4.7	11.9	−11.9	9.0
	MQC	8.6	4.6	4.3	5.4	–	4.2	7.3	−4.5	8.2	3.8	9.8
	HQC	7.7	4.0	12.5	1.7	3.1	12.2	2.2	−9.1	2.9	12.5	9.8
Bosutinib	LLOQ	1.3	7.1	5.0	6.2	–	–	–	–	–	–	–
	LQC	4.8	7.1	−11.7	10.2	9.9	0.1	7.1	−5.7	6.4	−1.2	12.2
	MQC	2.5	5.0	−12.6	9.2	–	2.3	2.3	−10.7	4.8	0.1	13.2
	HQC	−0.8	3.1	−4.0	7.5	7.8	13.3	3.1	−7.5	8.2	11.5	4.7
Dacomitinib	LLOQ	3.1	14.8	13.6	10.5	–	–	–	–	–	–	–
	LQC	12.1	10.9	−3.8	13.1	13.3	−7.1	4.4	−23.2	17.5	−5.8	11.3
	MQC	4.9	5.7	−0.04	5.8	–	−4.0	6.7	−0.8	10.3	−7.3	13.0
	HQC	0.8	3.7	7.0	2.8	5.5	7.5	0.7	−6.1	3.8	13.2	8.4
Dasatinib	LLOQ	−5.0	11.6	−1.8	4.3	–	–	–	–	–	–	–
	LQC	−1.7	4.2	−9.7	5.2	9.9	−8.0	11.1	−7.4	11.8	1.2	1.4
	MQC	3.6	4.8	−0.9	3.5	–	6.2	4.2	−11.9	3.4	−0.5	8.5
	HQC	4.4	3.0	10.8	2.5	12.3	−1.0	7.7	−1.8	4.5	−3.8	10.9
Erlotinib	LLOQ	1.2	3.1	−1.3	7.0	–	–	–	–	–	–	–
	LQC	6.8	2.2	4.3	2.7	7.3	1.9	5.7	4.0	3.9	9.2	2.9
	MQC	1.3	4.0	4.8	3.8	–	7.5	3.5	1.5	4.7	10.7	11.0
	HQC	−5.1	2.7	8.0	1.0	2.2	10.4	1.8	−7.1	4.6	11.5	1.2
Gefitinib	LLOQ	−2.5	13.7	−11.8	2.5	–	–	–	–	–	–	–
	LQC	4.1	4.1	−12.3	5.5	10.0	−8.4	2.9	−1.2	7.0	−13.6	8.5
	MQC	−0.2	4.2	−5.4	4.9	–	−1.7	2.1	−10.0	5.5	2.6	14.0
	HQC	−0.2	3.4	4.0	2.7	1.4	9.7	0.8	−12.6	4.7	12.9	1.7
Ibrutinib	LLOQ	6.9	4.0	−1.8	5.8	–	–	–	–	–	–	–
	LQC	−9.2	8.8	−6.4	3.2	10.2	−8.8	11.6	−11.2	6.8	−3.3	14.2
	MQC	9.1	4.1	8.5	7.2	–	−3.0	3.8	−10.6	10.3	−3.5	1.1
	HQC	10.2	2.1	13.6	1.6	7.7	3.3	4.8	−12.5	0.7	9.4	3.1
Imatinib	LLOQ	−2.3	19.1	−5.8	6.0	–	–	–	–	–	–	–
	LQC	13.4	2.6	1.1	0.9	12.1	5.0	7.6	9.6	11.7	14.2	8.7
	MQC	−3.7	2.5	−3.1	9.2	–	13.4	1.7	6.9	6.2	−9.7	8.4
	HQC	10.2	2.1	−1.7	4.8	11.8	11.6	6.0	−11.3	4.8	−9.5	7.6
Lapatinib	LLOQ	−1.4	5.1	3.7	13.3	–	–	–	–	–	–	–
	LQC	1.2	3.3	−3.2	5.8	11.8	−10.0	9.5	−2.9	7.0	−2.8	5.4
	MQC	9.3	3.1	0.4	9.1	–	−3.5	3.0	−6.4	3.5	−1.5	4.4
	HQC	3.1	3.4	13.0	0.9	3.4	14.6	2.4	−13.7	2.7	6.9	1.1
Lenvatinib	LLOQ	−1.4	5.1	7.8	8.5	–	–	–	–	–	–	–
	LQC	5.0	6.3	5.6	4.5	8.8	0.9	13.5	−2.9	7.0	−0.3	7.0
	MQC	5.2	3.6	4.2	6.0	–	−0.3	2.5	−6.3	5.7	12.4	12.4
	HQC	0.1	2.5	12.6	4.5	4.4	14.6	4.2	−12.5	1.9	14.3	5.6
Nilotinib	LLOQ	0.8	10.4	−1.3	13.0	–	–	–	–	–	–	–
	LQC	3.4	4.8	−3.4	13.4	12.8	8.2	10.2	5.6	10.9	13.3	5.6
	MQC	2.6	4.8	−8.8	9.4	–	−5.3	6.8	−4.0	5.4	−4.4	12.3
	HQC	−4.3	2.1	−4.2	10.1	10.4	−8.2	6.6	−11.6	3.0	−0.5	3.0
Nintedanib	LLOQ	0.7	8.2	4.4	18.8	–	–	–	–	–	–	–
	LQC	−1.0	8.3	−8.2	9.2	13.7	−11.7	2.8	−13.0	7.6	−9.5	12.0
	MQC	8.4	4.8	−4.2	10.5	–	−10.8	7.4	−12.3	5.8	−1.7	10.9
	HQC	3.4	3.6	1.7	10.4	8.4	−10.1	8.4	−8.9	2.6	10.4	3.8
Osimertinib	LLOQ	6.8	9.9	−2.3	3.5	–	–	–	–	–	–	–
	LQC	−6.5	9.0	−4.5	1.9	11.5	−24.6	9.1	−10.1	3.7	−13.6	7.4
	MQC	5.3	5.5	2.1	4.0	–	−8.3	4.5	−10.9	5.1	−3.3	4.9
	HQC	3.8	3.7	12.4	1.4	3.1	−9.2	4.0	−8.2	7.5	10.5	0.9
Pazopanib	LLOQ	−2.0	9.1	2.1	3.6	–	–	–	–	–	–	–
	LQC	−2.9	5.0	10.6	4.4	10.3	14.0	11.9	−15.7	5.2	13.0	5.7
	MQC	−7.8	3.1	−4.5	8.9	–	−9.7	2.9	−14.7	1.7	−6.8	8.4
	HQC	−11.1	2.6	2.7	5.1	5.5	−5.7	3.7	−13.0	1.7	−0.9	1.5
Ponatinib	LLOQ	−11.6	14.8	7.1	13.9	–	–	–	–	–	–	–
	LQC	−3.3	6.8	−6.9	4.4	6.4	−4.4	3.4	−12.1	10.7	−6.6	10.1
	MQC	8.7	5.2	1.9	9.2	–	−3.1	8.4	−10.2	8.3	−1.9	2.7
	HQC	8.0	3.9	12.2	2.1	4.5	13.6	2.1	−5.0	4.5	14.1	3.7

(*continued on next page*)

Table 5 (*continued*)

Analytes	Control samples	Intra-day		Inter-day		Matrix effect	25 °C, 4 h		4 °C, 24 h		3 times Freeze-thaw	
		RE (%)	CV (%)	RE (%)	CV (%)	CV (%)	RE (%)	CV (%)	RE (%)	CV (%)	RE (%)	CV (%)
Regorafenib	LLOQ	−6.8	4.1	−10.1	6.7	–	–	–	–	–	–	–
	LQC	−0.8	3.5	−8.1	5.0	11.3	−8.7	6.2	−4.8	11.1	6.6	6.6
	MQC	−2.4	3.7	0.4	7.8	–	−13.1	5.3	−11.1	5.1	−6.4	12.4
	HQC	−7.0	3.2	10.3	4.8	4.7	−8.1	6.6	−14.1	2.3	6.4	6.7
Sorafenib	LLOQ	−4.9	9.2	−3.7	9.0	–	–	–	–	–	–	–
	LQC	5.6	4.3	−4.5	6.0	12.8	−1.8	4.6	−2.8	9.6	7.1	8.5
	MQC	5.5	5.1	−3.1	7.5	–	−7.1	4.7	−9.6	7.7	−6.1	13.9
	HQC	−1.3	2.7	5.2	8.1	4.3	−0.9	3.8	−11.5	3.9	−2.8	2.6
Sunitinib	LLOQ	0.5	5.3	7.8	4.8	–	–	–	–	–	–	–
	LQC	1.5	3.8	−6.1	6.0	11.1	−12.5	9.4	−6.5	9.4	−7.03	4.6
	MQC	13.8	4.7	0.2	6.6	–	−10.9	5.4	−4.3	4.2	−13.7	8.0
	HQC	12.0	3.9	8.0	2.7	5.5	−2.2	1.9	0.6	4.2	−3.7	1.6
N-Desethyl sunitinib	LLOQ	1.3	6.7	−3.3	2.6	–	–	–	–	–	–	–
	LQC	5.9	3.4	−0.7	4.5	7.9	−12.9	3.4	−4.7	7.1	−14.2	4.0
	MQC	13.6	3.5	7.4	9.3	–	2.3	5.1	−4.5	8.6	−4.2	10.7
	HQC	5.9	3.5	8.1	2.0	6.4	0.1	3.7	−9.1	2.9	−0.6	2.0
Vandetanib	LLOQ	−6.3	7.4	−1.0	4.4	–	–	–	–	–	–	–
	LQC	−1.8	5.7	6.3	5.5	9.0	−13.8	2.5	−14.7	5.0	−10.7	6.6
	MQC	7.1	4.6	−7.1	8.6	–	−4.5	4.1	−12.1	6.4	−9.0	5.2
	HQC	0.2	3.1	−5.0	6.9	6.0	3.7	4.7	−10.2	5.2	3.2	5.1

RE, relative error; CV, coefficient of variation; LLOQ, lower limit of quantification; LQC, Low quality control; MQC, Medium quality control; HQC, High quality control.

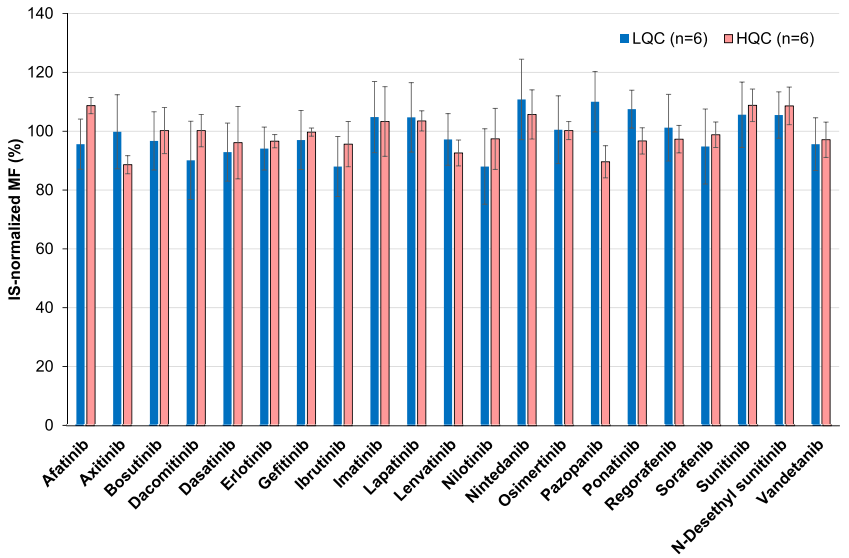

Fig. 3. Matrix factors of 20 oral molecular-targeted anticancer drugs and the active metabolite of sunitinib (n = 6). The horizontal axis shows each drug, and the vertical axis shows the IS normalized matrix factor.

4. Conclusion

High throughput LC/ESI-MS/MS method was developed for the simultaneous analysis of 20 oral molecular-targeted anticancer drugs and the active metabolite of sunitinib in human plasma using in-source CID, *s*-SRM, and *i*-SRM technique. This is the first simultaneous quantification method for drugs, such as ibrutinib and pazopanib, which have a large difference of more than 100,000-fold in the required concentration range. The validated method was successfully applied to the human plasma and was used for accurate measurement of the concentration of these drugs in patient samples. This analytical method can be applied to TDM of a wide range of oral molecular-targeted anticancer drugs in cancer genomic medicine and is expected to make a substantial contribution to the promotion of personalized medicine in the future.

Table 6
Concentrations of oral molecular-targeted anticancer drugs in the plasma of patients with cancer (n = 3).

Analytes	Gender	Drug regimen	Time of collecting blood	Concentration (ng/mL)
Axitinib	Female	6 mg, BID (After breakfast and dinner)	6:00	3.2
Axitinib	Male	10 mg, BID (After breakfast and dinner)	6:00	20.5
Bosutinib	Female	400 mg, QD (After breakfast)	9:00	275.1
Dasatinib	Female	100 mg, QD (After breakfast)	10:30	106.3
Ibrutinib	Male	420 mg, QD (After breakfast)	12:30	29.5
Imatinib	Male	300 mg, QD (After breakfast)	10:30	1046.7
Lenvatinib	Male	12 mg, QD (After dinner)	8:30	105.7
Nilotinib	Female	300 mg, BID (On an empty stomach)	12:30	713.7
Pazopanib	Male	400 mg, QD (2 h after breakfast)	6:00	41,644.8
Sorafenib	Male	600 mg, QD (After breakfast)	6:00	691.3
Sunitinib	Female	25 mg, QD (After breakfast)	6:00	42.3
N-Desethyl sunitinib	Female	25 mg, QD (After breakfast)	6:00	18.9

QD, once daily; BID, twice daily.

Author contribution statement

Tensei Hirasawa: Conceived and designed the experiments; Performed the experiments; Analyzed and interpreted the data; Wrote the paper.

Shinya Takasaki: Conceived and designed the experiments; Wrote the paper.

Masaki Kumondai, Yu Sato, Toshihiro Sato: Analyzed and interpreted the data.

Eishi Imoto, Yoshihiro Hayakawa:Contributed reagents, materials, analysis tools or data.

Masamitsu Maekawa, Nariyasu Mano: Conceived and designed the experiments; Analyzed and interpreted the data; Wrote the paper.

Masafumi Kikuchi: Conceived and designed the experiments; Performed the experiments; Analyzed and interpreted the data; Contributed reagents, materials, analysis tools or data; Wrote the paper.

Data availability statement

Data will be made available on request.

Declaration of competing interest

The authors declare that they have no known competing financial interests or personal relationships that could have appeared to influence the work reported in this paper.

Acknowledgments

This work was supported by JSPS KAKENHI Grant Number JP21K06708. We would like to thank Editage (www.editage.com) for the English language editing.

Appendix A. Supplementary data

Supplementary data to this article can be found online at https://doi.org/10.1016/j.heliyon.2023.e16926.

References

[1] S.L. Groenland, R.H.J. Mathijssen, J.H. Beijnen, A.D.R. Huitema, N. Steeghs, Individualized dosing of oral targeted therapies in oncology is crucial in the era of precision medicine, Eur. J. Clin. Pharmacol. 75 (2019) 1309–1318.

[2] K. Shiraishi, Y. Okada, A. Takahashi, Y. Kamatani, Y. Momozawa, K. Ashikawa, H. Kunitoh, S. Matsumoto, A. Takano, K. Shimizu, A. Goto, K. Tsuta, S. I. Watanabe, Y. Ohe, Y. Watanabe, Y. Goto, H. Nokihara, K. Furuta, A. Yoshida, K. Goto, T. Hishida, M. Tsuboi, K. Tsuchihara, Y. Miyagi, H. Nakayama, T. Yokose, K. Tanaka, T. Nagashima, Y. Ohtaki, D. Maeda, K. Imai, Y. Minamiya, H. Sakamoto, A. Saito, Y. Shimada, K. Sunami, M. Saito, J. Inazawa, Y. Nakamura, T. Yoshida, J. Yokota, F. Matsuda, K. Matsuo, Y. Daigo, M. Kubo, T. Kohno, Association of variations in HLA class II and other loci with susceptibility to EGFR-mutated lung adenocarcinoma, Nat. Commun. 7 (2016), 12451.

[3] M.G. Kris, B.E. Johnson, L.D. Berry, D.J. Kwiatkowski, A.J. Iafrate, Wistuba II, M. Varella-Garcia, W.A. Franklin, S.L. Aronson, P.F. Su, Y. Shyr, D.R. Camidge, L. V. Sequist, B.S. Glisson, F.R. Khuri, E.B. Garon, W. Pao, C. Rudin, J. Schiller, E.B. Haura, M. Socinski, K. Shirai, H. Chen, G. Giaccone, M. Ladanyi, K. Kugler, J. D. Minna, P.A. Bunn, Using multiplexed assays of oncogenic drivers in lung cancers to select targeted drugs, JAMA 311 (2014) 1998–2006.

[4] L. Zhong, Y. Li, L. Xiong, W. Wang, M. Wu, T. Yuan, W. Yang, C. Tian, Z. Miao, T. Wang, S. Yang, Small molecules in targeted cancer therapy: advances, challenges, and future perspectives, Signal Transduct. Targeted Ther. 6 (2021) 201.

[5] D.R. Spigel, H.A. Burris 3rd, F.A. Greco, D.L. Shipley, E.K. Friedman, D.M. Waterhouse, R.C. Whorf, R.B. Mitchell, D.B. Daniel, J. Zangmeister, J.D. Bass, J. D. Hainsworth, Randomized, double-blind, placebo-controlled, phase II trial of sorafenib and erlotinib or erlotinib alone in previously treated advanced non-small-cell lung cancer, J. Clin. Oncol. 29 (2011) 2582–2589.
[6] G.V. Scagliotti, M. Krzakowski, A. Szczesna, J. Strausz, A. Makhson, M. Reck, R.F. Wierzbicki, I. Albert, M. Thomas, J.E. Miziara, Z.S. Papai, N. Karaseva, S. Thongprasert, E.D. Portulas, J. von Pawel, K. Zhang, P. Selaru, L. Tye, R.C. Chao, R. Govindan, Sunitinib plus erlotinib versus placebo plus erlotinib in patients with previously treated advanced non-small-cell lung cancer: a phase III trial, J. Clin. Oncol. 30 (2012) 2070–2078.
[7] H. Jin, Y. Shi, Y. Lv, S. Yuan, C.F.A. Ramirez, C. Lieftink, L. Wang, S. Wang, C. Wang, M.H. Dias, F. Jochems, Y. Yang, A. Bosma, E.M. Hijmans, M.H.P. de Groot, S. Vegna, D. Cui, Y. Zhou, J. Ling, H. Wang, Y. Guo, X. Zheng, N. Isima, H. Wu, C. Sun, R.L. Beijersbergen, L. Akkari, W. Zhou, B. Zhai, W. Qin, R. Bernards, EGFR activation limits the response of liver cancer to lenvatinib, Nature 595 (2021) 730–734.
[8] L.V. Sequist, J.Y. Han, M.J. Ahn, B.C. Cho, H. Yu, S.W. Kim, J.C. Yang, J.S. Lee, W.C. Su, D. Kowalski, S. Orlov, M. Cantarini, R.B. Verheijen, A. Mellemgaard, L. Ottesen, P. Frewer, X. Ou, G. Oxnard, Osimertinib plus savolitinib in patients with EGFR mutation-positive, MET-amplified, non-small-cell lung cancer after progression on EGFR tyrosine kinase inhibitors: interim results from a multicentre, open-label, phase 1b study, Lancet Oncol. 21 (2020) 373–386.
[9] G.V. Long, K.T. Flaherty, D. Stroyakovskiy, H. Gogas, E. Levchenko, F. de Braud, J. Larkin, C. Garbe, T. Jouary, A. Hauschild, V. Chiarion-Sileni, C. Lebbe, M. Mandalà, M. Millward, A. Arance, I. Bondarenko, J.B.A.G. Haanen, J. Hansson, J. Utikal, V. Ferraresi, P. Mohr, V. Probachai, D. Schadendorf, P. Nathan, C. Robert, A. Ribas, M.A. Davies, S.R. Lane, J.J. Legos, B. Mookerjee, J.J. Grob, Dabrafenib plus trametinib versus dabrafenib monotherapy in patients with metastatic BRAF V600E/K-mutant melanoma: long-term survival and safety analysis of a phase 3 study, Ann. Oncol. 28 (2017) 1631–1639.
[10] B. Gao, S. Yeap, A. Clements, B. Balakrishnar, M. Wong, H. Gurney, Evidence for therapeutic drug monitoring of targeted anticancer therapies, J. Clin. Oncol. 30 (2012) 4017–4025.
[11] N. Widmer, C. Bardin, E. Chatelut, A. Paci, J. Beijnen, D. Levêque, G. Veal, A. Astier, Review of therapeutic drug monitoring of anticancer drugs part two–targeted therapies, Eur. J. Cancer 50 (2014) 2020–2036.
[12] N. Takahashi, H. Wakita, M. Miura, S.A. Scott, K. Nishii, M. Masuko, M. Sakai, Y. Maeda, K. Ishige, M. Kashimura, K. Fujikawa, M. Fukazawa, T. Katayama, F. Monma, M. Narita, F. Urase, T. Furukawa, Y. Miyazaki, N. Katayama, K. Sawada, Correlation between imatinib pharmacokinetics and clinical response in Japanese patients with chronic-phase chronic myeloid leukemia, Clin. Pharmacol. Ther. 88 (2010) 809–813.
[13] S. Picard, K. Titier, G. Etienne, E. Teilhet, D. Ducint, M.A. Bernard, R. Lassalle, G. Marit, J. Reiffers, B. Begaud, N. Moore, M. Molimard, F.X. Mahon, Trough imatinib plasma levels are associated with both cytogenetic and molecular responses to standard-dose imatinib in chronic myeloid leukemia, Blood 109 (2007) 3496–3499.
[14] R.B. Verheijen, H. Yu, J.H.M. Schellens, J.H. Beijnen, N. Steeghs, A.D.R. Huitema, Practical recommendations for therapeutic drug monitoring of kinase inhibitors in oncology, Clin. Pharmacol. Ther. 102 (2017) 765–776.
[15] M. Shipkova, D. Svinarov, LC-MS/MS as a tool for TDM services: where are we? Clin. Biochem. 49 (2016) 1009–1023.
[16] Y. Mukai, T. Yoshida, T. Kondo, N. Inotsume, T. Toda, Novel high-performance liquid chromatography-tandem mass spectrometry method for simultaneous quantification of BCR-ABL and Bruton's tyrosine kinase inhibitors and their three active metabolites in human plasma, J. Chromatogr., B: Anal. Technol. Biomed. Life Sci. 1137 (2020), 121928.
[17] D. Koller, V. Vaitsekhovich, C. Mba, J.L. Steegmann, P. Zubiaur, F. Abad-Santos, A. Wojnicz, Effective quantification of 11 tyrosine kinase inhibitors and caffeine in human plasma by validated LC-MS/MS method with potent phospholipids clean-up procedure. Application to therapeutic drug monitoring, Talanta 208 (2020), 120450.
[18] C. Merienne, M. Rousset, D. Ducint, N. Castaing, K. Titier, M. Molimard, S. Bouchet, High throughput routine determination of 17 tyrosine kinase inhibitors by LC-MS/MS, J. Pharm. Biomed. Anal. 150 (2018) 112–120.
[19] J. Shen, H. Wang, H. Huang, H. Li, C. Li, C. Yan, T. Yu, H. Guo, K. Hu, Y. Du, H. Sun, L. Xie, P. Fang, Y. Liang, Absolute quantitative analysis of endogenous neurotransmitters and amino acids by liquid chromatography-tandem mass spectrometry combined with multidimensional adsorption and collision energy defect, J. Chromatogr. A 1638 (2021), 461867.
[20] H. Ishii, M. Shimada, H. Yamaguchi, N. Mano, A simultaneous determination method for 5-fluorouracil and its metabolites in human plasma with linear range adjusted by in-source collision-induced dissociation using hydrophilic interaction liquid chromatography-electrospray ionization-tandem mass spectrometry, Biomed. Chromatogr. 30 (2016) 1882–1886.
[21] M.A. Curtis, L.C. Matassa, R. Demers, K. Fegan, Expanding the linear dynamic range in quantitative high performance liquid chromatography/tandem mass spectrometry by the use of multiple product ions, Rapid Commun. Mass Spectrom. 15 (2001) 963–968.
[22] H. Liu, L. Lam, P.K. Dasgupta, Expanding the linear dynamic range for multiple reaction monitoring in quantitative liquid chromatography-tandem mass spectrometry utilizing natural isotopologue transitions, Talanta 87 (2011) 307–310.
[23] M. Maekawa, T. Tsukamoto, S. Takasaki, M. Kikuchi, Y. Sato, J. Ogura, Y. Hayakawa, H. Yamaguchi, N. Mano, Fundamental study of behaviors of in-source collision induced dissociation and shifting the linear range of calibration curves of various drugs and the metabolites used for therapeutic drug monitoring, Chromatography 40 (2019) 71–78.
[24] S. Takasaki, T. Hirasawa, Y. Sato, M. Maekawa, T. Tsukamoto, M. Kikuchi, J. Ogura, Y. Hayakawa, Y. Matsuda, H. Oishi, T. Sado, M. Noda, Y. Okada, H. Yamaguchi, N. Mano, Simultaneous analysis of drugs administered to lung-transplanted patients using liquid chromatography-tandem mass spectrometry for therapeutic drug monitoring, Biomed. Chromatogr. 35 (2021) e5067.
[25] T. Sato, M. Suzuka, Y. Sato, R. Iwabuchi, D. Kobayashi, J. Ogura, S. Takasaki, M. Yokota, T. Tsukamoto, Y. Hayakawa, M. Kikuchi, M. Maekawa, N. Mano, Development of a simultaneous analytical method for clozapine and its metabolites in human plasma using liquid chromatography/electrospray ionization tandem mass spectrometry with linear range adjusted by in-source collision-induced dissociation, Biomed. Chromatogr. 35 (2021), e5094.
[26] T. Hirasawa, M. Kikuchi, K. Shigeta, S. Takasaki, Y. Sato, T. Sato, J. Ogura, K. Onodera, N. Fukuhara, Y. Onishi, M. Maekawa, N. Mano, High-throughput liquid chromatography/electrospray ionization-tandem mass spectrometry method using in-source collision-induced dissociation for simultaneous quantification of imatinib, dasatinib, bosutinib, nilotinib, and ibrutinib in human plasma, Biomed. Chromatogr. 35 (2021) e5124.
[27] Yu Sato, Kensuke Shigeta, Tensei Hirasawa, Toshihiro Sato, Jiro Ogura, Masamitsu Maekawa, Akiko Ebata, Yohei Hamanaka, Hiroshi Tada, Takanori Ishida, Masafumi Kikuchi, Nariyasu Mano, Establishment of an analytical method for simultaneous quantitation of CDK4/6 inhibitors, aromatase inhibitors, and an estrogen receptor antagonist in human plasma using LC-ESI-MS/MS, J. Chromatogr., B: Anal. Technol. Biomed. Life Sci. 1173 (2021), 122655.
[28] T. Hirasawa, M. Kikuchi, S. Takasaki, K. Masaki, Y. Sato, T. Sato, I. Eishi, H. Yoshihiro, M. Maekawa, N. Mano, Shifting the linear range of the calibration curves for the quantification of oral molecular-targeted anticancer drugs and the active metabolite in human plasma using LC-ESI-MS/MS, Med Mass Spectrometry 6 (2022) 52–63.
[29] U.S. Department of Health and Human Services, Food and Drug Administration, Bioanalytical Method Validation Guidance for Industry, 2018.
[30] A. Cipurković, S. Marić, E. Horozić, S. Hodžić, D. Husejnagić, L. Kolarević, A. Zukić, D. Bjelošević, Complexes of Co (II), Cu (II) and Ni (II) with antineoplastic agent imatinib mesylate : synthesis , characterization and biological activity, Am. J. Chem. 9 (2019) 159–164.
[31] Y. Moriiwa, N. Suzuki, A. Shoji, A. Yanagida, Analysis of complexation interactions between metal ions and drugs under pseudo-physiological pH conditions by a high-throughput screening method using a solid-phase extraction cartridge, Anal. Sci. 36 (2020) 709–715.
[32] R. Reis, L. Labat, M. Allard, P. Boudou-Rouquette, J. Chapron, A. Bellesoeur, A. Thomas-Schoemann, J. Arrondeau, F. Giraud, J. Alexandre, M. Vidal, F. Goldwasser, B. Blanchet, Liquid chromatography-tandem mass spectrometric assay for therapeutic drug monitoring of the EGFR inhibitors afatinib, erlotinib and osimertinib, the ALK inhibitor crizotinib and the VEGFR inhibitor nintedanib in human plasma from non-small cell lung cancer patients, J. Pharm. Biomed. Anal. 158 (2018) 174–183.
[33] G.D.M. Veerman, M.H. Lam, R.H.J. Mathijssen, S.L.W. Koolen, P. de Bruijn, Quantification of afatinib, alectinib, crizotinib and osimertinib in human plasma by liquid chromatography/triple-quadrupole mass spectrometry; focusing on the stability of osimertinib, J. Chromatogr., B: Anal. Technol. Biomed. Life Sci. 1113 (2019) 37–44.
[34] A. van Veelen, R. van Geel, Y. de Beer, A.M. Dingemans, L. Stolk, R. Ter Heine, F. de Vries, S. Croes, Validation of an analytical method using HPLC-MS/MS to quantify osimertinib in human plasma and supplementary stability results, Biomed. Chromatogr. 34 (2020), e4771.

[35] M. Mžik, N. Váňová, M. Kriegelstein, M. Hroch, Differential adsorption of an analyte and its D4, D5 and 13C6 labeled analogues combined with instrument-specific carry-over issues: the Achilles' heel of ibrutinib TDM, J. Pharm. Biomed. Anal. 206 (2021), 114366.
[36] E.P. Hui, B.B.Y. Ma, H.H.F. Loong, F. Mo, L. Li, A.D. King, K. Wang, A.T. Ahuja, C.M.L. Chan, C.W.C. Hui, C.H. Wong, A.T.C. Chan, Efficacy, safety, and pharmacokinetics of axitinib in nasopharyngeal carcinoma: a preclinical and phase II correlative study, Clin. Cancer Res. 24 (2018) 1030–1037.
[37] A. Inoue, C.K. Imamura, H. Shimada, D. Katayama, K. Urabe, R. Suzuki, K. Takitani, A. Ashida, Pharmacokinetics, efficacy and safety of bosutinib in a pediatric patient with chronic myeloid leukemia, J. Pediatr. Pharmacol. Therapeut. 25 (2020) 742–745.
[38] J. Mori, K. Oshima, T. Tanimoto, H. Ishizuka, S. Kimura, M. Miura, N. Takahashi, Pharmacokinetics of dasatinib in a hemodialysis patient with chronic myeloid leukemia and chronic kidney disease, Int. J. Hematol. 112 (2020) 115–117.
[39] C.M. Vela, A. McBride, S.M. Jaglowski, L.A. Andritsos, Ibrutinib for treatment of chronic lymphocytic leukemia, Am. J. Health Syst. Pharm. 73 (2016) 367–375.
[40] H.P. Gschwind, U. Pfaar, F. Waldmeier, M. Zollinger, C. Sayer, P. Zbinden, M. Hayes, R. Pokorny, M. Seiberling, M. Ben-Am, B. Peng, G. Gross, Metabolism and disposition of imatinib mesylate in healthy volunteers, Drug Metab. Dispos. 33 (2005) 1503–1512.
[41] D. Liu, L. Liu, L. Shen, T. Kubota, T. Suzuki, H. Ikezawa, S. Shiba, Y. Bai, Pharmacokinetic study of lenvatinib in Chinese patients with solid tumors, Future Oncol. 17 (2021) 1855–1863.
[42] N. Hijiya, C.M. Zwaan, C. Rizzari, R. Foà, F. Abbink, D. Lancaster, J. Landman-Parker, F. Millot, J. Moppett, B. Nelken, M. Caterina Putti, X. Tian, K. Sinclair, H. Santanastasio, A. Buchbinder, P. Kearns, Pharmacokinetics of nilotinib in pediatric patients with philadelphia chromosome-positive chronic myeloid leukemia or acute lymphoblastic leukemia, Clin. Cancer Res. 26 (2020) 812–820.
[43] R.B. Verheijen, J.H. Beijnen, J.H.M. Schellens, A.D.R. Huitema, N. Steeghs, Clinical pharmacokinetics and pharmacodynamics of pazopanib: towards optimized dosing, Clin. Pharmacokinet. 56 (2017) 987–997.
[44] L. Jain, S. Woo, E.R. Gardner, W.L. Dahut, E.C. Kohn, S. Kummar, D.R. Mould, G. Giaccone, R. Yarchoan, J. Venitz, W.D. Figg, Population pharmacokinetic analysis of sorafenib in patients with solid tumours, Br. J. Clin. Pharmacol. 72 (2011) 294–305.
[45] E. Wang, S.G. DuBois, C. Wetmore, R. Khosravan, Population pharmacokinetics-pharmacodynamics of sunitinib in pediatric patients with solid tumors, Cancer Chemother. Pharmacol. 86 (2020) 181–192.